Article

# Small-Molecule Dynamics and Mechanisms Underlying the Macroscopic Mechanical Properties of Coordinatively Cross-Linked Polymer Networks

Wayne C. Yount, David M. Loveless, and Stephen L. Craig

*J. Am. Chem. Soc.*, **2005**, 127 (41), 14488-14496• DOI: 10.1021/ja054298a • Publication Date (Web): 22 September 2005



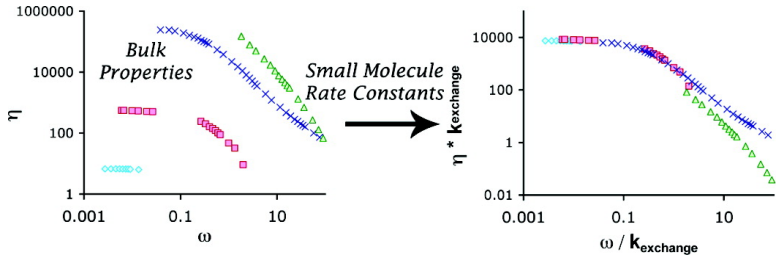


## More About This Article

Additional resources and features associated with this article are available within the HTML version:

- Supporting Information
- Links to the 6 articles that cite this article, as of the time of this article download
- Access to high resolution figures
- Links to articles and content related to this article
- Copyright permission to reproduce figures and/or text from this article

View the Full Text HTML

J|A|C|S
ARTICLES
Published on Web 09/22/2005

# Small-Molecule Dynamics and Mechanisms Underlying the Macroscopic Mechanical Properties of Coordinatively Cross-Linked Polymer Networks

Wayne C. Yount, David M. Loveless, and Stephen L. Craig*

*Contribution from the Department of Chemistry and Center for Biologically Inspired Materials and Material Systems, Duke University, Durham, North Carolina 27708-0346*

Received June 29, 2005; E-mail: stephen.craig@duke.edu

***Abstract:*** Specific metal−ligand coordination between bis-Pd(II) and Pt(II) organometallic cross-linkers and poly(4-vinylpyridine) in DMSO defines a three-dimensional associative polymer network. Frequency-dependent dynamic mechanical moduli of a series of four different bulk materials, measured across several decades of oscillatory strain rates, are found to be quantitatively related through the pyridine exchange rates measured on model Pd(II) and Pt(II) complexes. Importantly, the mechanism of ligand exchange in the networks is found to be the same solvent-assisted pathway observed in the model complexes, and so the bulk mechanical properties are determined by relaxations that occur when the cross-links are dissociated from the polymer backbone. It is how often the cross-links dissociate, independently of how long they remain dissociated, that determines the bulk mechanical properties. The quantitative relationship between bulk materials properties and the kinetics and mechanisms observed in model compounds holds promise for the rational, molecular design of materials with tailored mechanical properties.

## Introduction

A small-molecule perspective is becoming increasingly common and productive in the design of bulk materials. A primary driver of this movement is the profitable use of reversible self-assembly, in which specific and well-defined interactions between molecules define structure on mesoscopic and macroscopic length scales. The advantages of the self-assembly approach lie in the dynamic nature of the supramolecular structure. Whereas the covalent structure of a molecule is effectively fixed, intermolecular interactions are relatively pliable. The supramolecular properties are therefore environmentally responsive in a way that permits tunable and reversible materials. The growing list of responsive, supramolecular materials includes polymers,[1−8] strong and weak organogels,[9−12] amphiphilic assemblies,[13−16] and liquid crystals.[17] In these and related materials, material properties are closely tied to the structure of small molecules. As the relationship between molecular and material properties becomes more clearly defined, the ability to control material properties through the synthetic manipulation of the molecular component increases.

In general, a rational, molecular design of materials should be based on a quantitative and sophisticated understanding of molecule-to-material relationships in two regimes: structure and dynamics. Within supramolecular approaches to materials, it is the structural aspect that has received the most attention and for which a strong mechanistic base has been laid. The dynamic nature of the defining interactions, however, is often the attribute that distinguishes supramolecular materials from their covalent counterparts.[18] Those dynamics are often central to the function of the material; they govern how the structure and properties of the material evolve in response to environmental changes such as mechanical stress, temperature, or chemical potential. Dynamics therefore determine the mechanical properties of a material, and they also dictate the time scale of sensing and switching in devices. Despite their significance, direct and quantitative mechanistic studies of the molecular contributions to the dynamic properties of materials are far less common than are structural investigations.[19,20]

(1) Ciferri, A. *Supramolecular Polymers*; Marcel Dekker: New York, 1998.
(2) Brunsveld, L.; Folmer, B. J. B.; Meijer, E. W.; Sijbesman, R. P. *Chem. Rev.* **2001**, *101*, 4071−4097.
(3) Sijbesma, R. P.; Beijer, F. H.; Brunsveld, L.; Folmer, B. J. B.; Hirschberg, J. H. K. K.; Lange, R. F. M.; Lowe, J. K. L.; Meijer, E. W. *Science* **1997**, *278*, 1601−1604.
(4) Schubert, U. S.; Hofmeier, H. *Macromol. Rapid Commun.* **2002**, *23*, 561−566.
(5) Pollino, J. M.; Nair, K. P.; Stubbs, L. P.; Adams, J.; Weck, M. *Tetrahedron* **2004**, *60*, 7205−7215.
(6) Rowan, S. J.; Beck, J. B.; Ineman, J. M. *Polym. Prepr. (Am. Chem. Soc., Div. Polym. Chem.)* **2003**, *44*, 691−692.
(7) Castellano, R. K.; Clark, R.; Craig, S. L.; Nuckolls, C.; Rebek, J., Jr. *Proc. Natl. Acad. Sci. U.S.A.* **2000**, *97*, 12418−12421.
(8) Kato, T.; Fréchet, J. M. J. *J. Am. Chem. Soc.* **1989**, *111*, 8533−8534.
(9) Terech, P.; Weiss, R. G. *Chem. Rev.* **1997**, *97*, 3133−3159.
(10) Estroff, L. A.; Hamilton, A. D. *Chem. Rev.* **2004**, *104*, 1201−1217.
(11) Willemen, H. M.; Vermonden, T.; Marcelis, A. T. M.; Sudhölter, E. J. R. *Langmuir* **2002**, *18*, 7102−7106.
(12) Willemen, H. M.; Marcelis, A. T. M.; Sudhölter, E. J. R.; Bouwman, W. G.; Deme, B.; Terech, P. *Langmuir* **2004**, *20*, 2075−2080.
(13) Gohy, J.-F.; Lohmeijer, B. G. G.; Varshney, S. K.; Schubert, U. S. *Macromolecules* **2002**, *35*, 7427−7435.
(14) Drechsler, U.; Thibault, R. J.; Rotello, V. M. *Macromolecules* **2002**, *35*, 9621−9623.
(15) Tang, X.; Hua, F.; Yamato, K.; Ruckenstein, E.; Gong, B.; Kim, W.; Ryu, C. Y. *Angew. Chem., Int. Ed.* **2004**, *43*, 6471−6474.
(16) Liu, Y.; Xu, J.; Craig, S. L. *Chem. Commun.* **2004**, 1864−1865.
(17) Percec, V. *Macromol. Symp.* **1997**, *117*, 267−273.
(18) Davis, A. V.; Yeh, R. M.; Raymond, K. N. *Proc. Natl. Acad. Sci. U.S.A.* **2002**, *99*, 4793−4796.
(19) Davis, J. T.; Kaucher, M. S.; Kotch, F. W.; Iezzi, M. A.; Clover, B. C.; Mullaugh, K. M. *Org. Lett.* **2004**, *6*, 4265−4268.


**10.1021/ja054298a CCC: $30.25** 

The importance of supramolecular dynamics is not limited to materials,[21−25] and recent work has demonstrated the role of molecular dynamics in catalysis,[21−25] templation effects,[26,27] interconversion of assemblies,[26,28] and kinetic compartmentalization.[29,30] Davis et al.[18] and Bohne and co-workers,[31−34] in particular, have noted the difficulties that are common to experimental investigations of dynamics in supramolecular chemistry. These difficulties in characterization include the structural ambiguity that is inherent in large assemblies, the fact that the dynamics of the "cause" (individual molecular associations) can be several orders of magnitude faster than those of the "effect" (dynamic property of the assembly), and the technical challenge of observing and quantifying the dynamics of individual molecular interactions within a material superstructure.

Our interest stems from the use of reversible, supramolecular interactions as a defining element in polymeric materials. By "defining element", we mean that, in the absence of the interactions, the molecules under investigation are too small to be physically entangled or to bridge between surfaces,[35−37] two common polymeric mechanisms for transducing force. When the reversible interactions are considered, however, the supramolecular structures are sufficiently large that these mechanisms become accessible, and mechanical properties might be enhanced. The physics of the supramolecular polymer and mechanical properties of the material are then intrinsically and closely tied to very specific intermolecular interactions. In these materials, an understanding of fundamental behaviors requires as much of a small-molecule perspective as it does a macromolecular one.

Areas of interest include linear supramolecular polymers (SPs),[3,13,38−58] in which specific, reversible interactions define the main chain of a linear polymer, and SP networks (Figure 1a), in which the reversible interactions define a contiguous three-dimensional topology. The SP networks are technically a subset of physical gels, in which covalent chains are transiently cross-linked by reversible interactions, and their technical appeal includes mechanical properties and stability that are easily tailored and stimuli-responsive. The motifs employed as specific

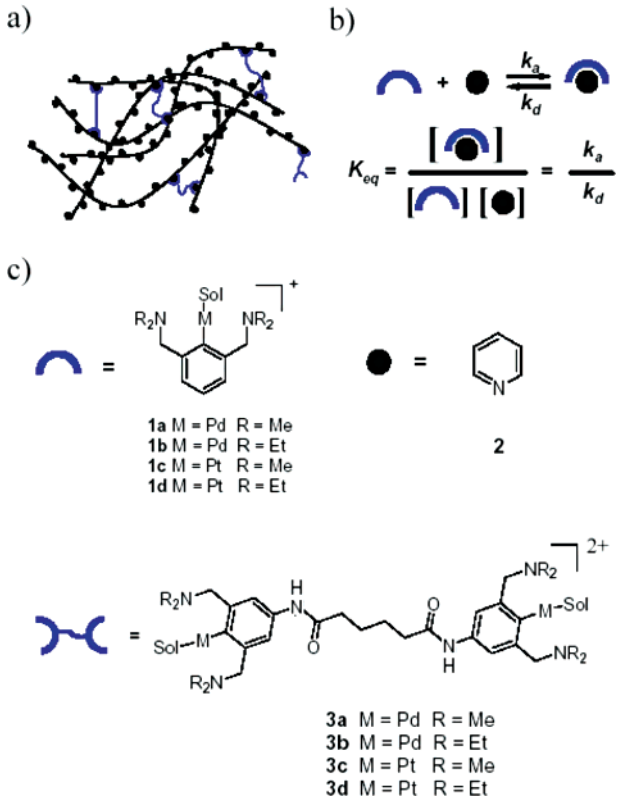


***Figure 1.*** (a) Schematic of a supramolecular polymer network in which polymer side chains are cross-linked by bisfunctional recognition units. (b) Thermodynamic and kinetic parameters of the supramolecular interaction underlying network formation. (c) Molecular structures employed in this work; triflate counterions not pictured.

(20) Hori, A.; Yamashita, K.; Fujita, M. *Angew. Chem., Int. Ed.* **2004**, *43*, 5016−5019.
(21) Ziegler, M.; Brumanghim, J. L.; Raymond, K. N. *Angew. Chem., Intl. Ed.* **2000**, *39*, 4119−4121.
(22) Kang, J.; Rebek, J., Jr. *Nature* **1997**, *385*, 50−52.
(23) Kang, J.; Santamaria, J.; Hilmersson, G.; Rebek, J., Jr. *J. Am. Chem. Soc.* **1998**, *120*, 7389−7390.
(24) Kang, J.; Hilmersson, G.; Santamaria, J.; Rebek, J., Jr. *J. Am. Chem. Soc.* **1998**, *120*, 3650−3656.
(25) Yoshizawa, M.; Kusukawa, T.; Fujita, M.; Sakamoto, S.; Yamaguchi, K. *J. Am. Chem. Soc.* **2001**, *122*, 10454−10459.
(26) Scherer, M.; Caulder, D. L.; Johnson, D. W.; Raymond, K. N. *Angew. Chem., Int. Ed.* **1999**, *38*, 1588−1592.
(27) Rivera, J.; Craig, S. L.; Martin, T.; Rebek, J., Jr. *Angew. Chem., Int. Ed.* **2000**, *12*, 3986−3988.
(28) Kersting, B.; Telford, J. R.; Meyer, M.; Raymond, K. N. *J. Am. Chem. Soc.* **1996**, *118*, 7221−7222.
(29) Körner, S.; Chen, J.; Craig, S. L.; Rudkevich, D.; Rebek, J., Jr. *Nature* **2002**, *415*, 385−386.
(30) Chen, J.; Körner, S.; Craig, S. L.; Lin, S.; Rudkevich, D.; Rebek, J., Jr. *Proc. Natl. Acad. Sci. U.S.A.* **2002**, *99*, 2593−2596.
(31) Bohne, C. *Spectrum* **2000**, *13*, 14−19.
(32) Dyck, A. S. M.; Kisiel, U.; Bohne, C. *J. Phys. Chem. B* **2003**, *107*, 11652−11659.
(33) Okano, L. T.; Barros, T. C.; Chou, D. T. H.; Bennet, A. J.; Bohne, C. *J. Phys. Chem. B* **2001**, *105*, 2122−2128.
(34) Rinco, O.; Nolet, M.-C.; Ovans, R.; Bohne, C. *Photochem. Photobiol. Sci.* **2003**, *2*, 1140−1151.
(35) Kim, J.; Liu, Y.; Ahn, S. J.; Zauscher, S.; Karty, J. M.; Yamanaka, Y.; Craig, S. L. *Adv. Mater.* **2005**, *17*, 1749−1753.
(36) Kersey, F. R.; Lee, G.; Marszalek, P.; Craig, S. L. *J. Am. Chem. Soc.* **2004**, *126*, 3038−3039.
(37) Zou, S.; Schonherr, H.; Vancso, G. J. *Angew. Chem., Int. Ed.* **2005**, *44*, 956−959.
(38) Lehn, J.-M. *Makromol. Chem., Macromol. Symp.* **1993**, *69*, 1−17.
(39) Hilger, C.; Stadler, R. *Makromol. Chem.* **1991**, *192*, 805−817.
(40) Dankers, P. Y. W.; van Beek, D. J. M.; ten Cate, A. T.; Sijbesma, R. P.; Meijer, E. W. *Polym. Mater. Sci. Eng.* **2003**, *88*, 52−53.
(41) ten Cate, A. T.; van Beek, D. J. M.; Spiering, A. J. H.; Dankers, P. Y. W.; Sijbesma, R. P.; Meijer, E. W. *Polym. Prepr. (Am. Chem. Soc., Div. Polym. Chem.)* **2003**, *44*, 618−619.
(42) Hirschberg, J. H. K. K.; Ramzi, A.; Sijbesma, R. P.; Meijer, E. W. *Macromolecules* **2003**, *36*, 1429−1432.
(43) Sijbesma, R. P.; Folmer, B. J. B.; Meijer, E. W. *Polym. Prepr. (Am. Chem. Soc., Div. Polym. Chem.)* **2002**, *43*, 375−376.
(44) Bosman, A. W.; Folmer, B. J. B.; Hirschberg, J. H. K. K.; Keizer, H. M.; Sijbesma, R. P.; Meijer, E. W. *Polym. Prepr. (Am. Chem. Soc., Div. Polym. Chem.)* **2002**, *43*, 322.
(45) Castellano, R. K.; Rudkevich, D. M.; Rebek, J., Jr. *Proc. Natl. Acad. Sci. U.S.A.* **1997**, *94*, 7132−7137.
(46) Knapp, R.; Schott, A.; Rehahn, M. *Macromolecules* **1996**, *29*, 478−480.
(47) Meier, M. A. R.; Schubert, U. S. *Polym. Mater. Sci. Eng.* **2003**, *88*, 443−444.
(48) Hofmeier, H.; Gohy, J.-F.; Schubert, U. S. *Polym. Mater. Sci. Eng.* **2003**, *88*, 193−194.
(49) Hofmeier, H.; El-Ghayoury, A.; Schubert, U. S. *Polym. Prepr. (Am. Chem. Soc., Div. Polym. Chem.)* **2003**, *44*, 711−712.
(50) Hofmeier, H.; Schmatloch, S.; Schubert, U. S. *Polym. Prepr. (Am. Chem. Soc., Div. Polym. Chem.)* **2003**, *44*, 709−710.
(51) Schmatloch, S.; Gonzalez, M. F.; Schubert, U. S. *Macromol. Rapid Commun.* **2002**, *23*, 957−961.
(52) Gohy, J.-F.; Lohmeijer, B. G. G.; Varshney, S. K.; Decamps, B.; Leroy, E.; Boileau, S.; Schubert, U. S. *Macromolecules* **2002**, *35*, 9748−9755.
(53) Lohmeijer, B. G. G.; Schubert, U. S. *Angew. Chem., Int. Ed.* **2002**, *41*, 3825−3829.
(54) Schubert, U. S.; Schmatloch, S.; Precup, A. A. *Des. Monomers Polym.* **2002**, *5*, 211−221.
(55) Schubert, U. S.; Eschbaumer, C. *Angew. Chem., Int. Ed.* **2002**, *41*, 2892−2926.
(56) Chen, C.-C.; Dormidontova, E. E. *J. Am. Chem. Soc* **2004**, *126*, 14972−14978.
(57) Fogleman, E. A.; Yount, W. C.; Xu, J.; Craig, S. L. *Angew. Chem., Int. Ed.* **2002**, *41*, 4026−4028.
(58) Xu, J.; Fogleman, E. A.; Craig, S. L. *Macromolecules* **2004**, *37*, 1863−1870.

cross-linking agents include hydrogen bonding, metal−ligand coordination, and salt bridges. Some recent designer networks include Beck and Rowan's multiply responsive lanthanide-based networks,[59] the cross-linked "universal polymer backbones" implemented by Pollino et al.,[5] and Vermonden et al.'s modular, neodymium-based coordination system.[60] These efforts are representative of the growing number of supramolecular approaches to material science, and they illustrate that the environmental and mechanical properties of SPs might be broadly suited to a range of materials applications, if the underlying molecular mechanisms of their properties were fully understood and exploited.

Whether in linear or networked SPs, the thermodynamics of the intermolecular interaction are often a primary consideration in SP design and discussion, but dynamics clearly play a role. The contributions of these molecular dynamics are particularly important under nonequilibrium conditions such as those imposed by a mechanical stress. Stress relaxation in networks and concentrated polymer solutions is dominated by the dynamics of the cross-links or entanglements between polymer chains. In SPs, relaxation of those entanglements might occur most rapidly through the dissociation and reassociation of the defining intermolecular interaction. The contributions of dynamic interactions to material properties have been considered primarily through one of two vehicles: extension of the transient network theory of Green and Tobolsky[61] to associative polymer networks and gels,[62−64] and Cates' theory of "living" polymer reptation derived initially in the context of wormlike micelles.[65−68] The theories are similar in that polymer mechanics are related to the dynamics of reversible molecular interactions, although in the Cates theory those dynamics create hybrid reptative relaxation pathways.[66,67]

To gain a molecular perspective on the underlying mechanisms of SP properties, we have employed the equivalent of a macromolecular "kinetic isotope effect", in that molecular contributions to rate-determining material processes are revealed by kinetic differences in two isostructural systems. The independent control of $k_d$ relative to $K_{eq}$ is accomplished through simple steric effects at the metal of square planar Pd(II) and Pt(II) complexes. Ligand exchange at square planar Pd(II) and Pt(II) typically occurs through an associative process, in which the attacking nucleophile associates to the metal center prior to the departure of the original ligand. Because the pentacoordinate transition state is crowded relative to the reactant and product metal−ligand complexes, steric effects in the spectator ligands of the complex have a significant effect on the rate of ligand exchange while having a minimal effect (by comparison to the transition state) on the stability of the isosteric endpoints. Pincer motifs such as those investigated extensively by van Koten and co-workers[69] have proven to be attractive in this regard (Figure 1c).[70,71] In addition to the ease of steric manipulation of the spectator ligands, the pincer complexes have the added advantage of increased stability, a particularly attractive feature given the moderate stability of many aryl Pd(II) organometallic complexes. Pincer alkylamine ligands were chosen for their synthetic accessibility and the demonstrated stability of reported complexes.[72] The pincer systems are also amenable to numerous structural modifications through the organometallic aryl group, metal, pincer ligands, counterion, and associating ligand. These modifications allow the motif to be tailored to numerous desired polymeric endpoints (e.g., solubility, variations in persistence length, and cohesive energy density). Depending on one's perspective,[73] the use of the term "supramolecular" may or may not be appropriate to the metal−ligand coordination employed here. For the purposes of this study, it is the specific, directional, and dynamic nature of the interactions that are important. Understanding the consequences of the interactions, regardless of their classification, on properties beyond the isolated molecules constitutes an objective that is often, although certainly not uniquely, described as "supramolecular", and the term is used here in that context.

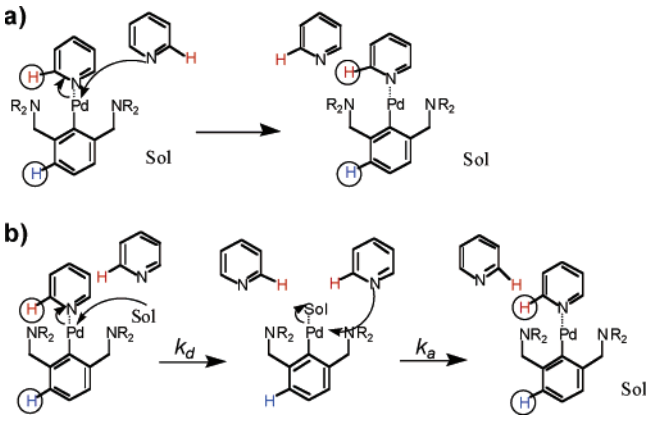


***Figure 2.*** Exchange mechanisms for pincer−pyridine complexes. Chemical exchange between complexed (circled) and free (not circled) states of red and blue hydrogens is monitored concurrently by spin magnetization transfer NMR. (a) Direct displacement of one pyridine by another pyridine. (b) Solvent-assisted ligand exchange.

We recently reported that bis-Pd(II) complexes **3a** and **3b** (Figure 1c) form cross-linked networks when mixed with poly(4-vinylpyridine) (PVP) in DMSO (Figure 3), and it was shown that the dynamics of the cross-linking associations are the primary determinants of bulk viscosity.[71] Here, we examine the scope of the molecule-to-material relationship in the frequency-dependent bulk dynamic mechanical properties of these SP networks, and we find that differences in properties that span several orders of magnitude are related rather precisely to a common master plot behavior through the small-molecule dynamics of the defining supramolecular cross-links. Further, the specific mechanisms underlying those dynamics in both the

(59) (a) Beck, J. B.; Rowan, S. J. *J. Am. Chem. Soc.* **2003**, *125*, 13922−13923. (b) Zhao, Y.; Beck, J. B.; Rowan, S. J.; Jamieson, A. M. *Macromolecules* **2004**, *37*, 3529−3531.
(60) Vermonden, T.; van Steenbergen, M. J.; Besseling, N. A. M.; Marcelis, A. T. M.; Hennink, W. E.; Sudhölter, E. J. R.; Cohen Stuart, M. A. *J. Am. Chem. Soc* **2004**, *126*, 15802−15808.
(61) Green, M. S.; Tobolsky, A. V. *J. Chem. Phys.* **1946**, *14*, 80−89.
(62) Yamamoto, M. *J. Phys. Soc. Jpn.* **1956**, *11*, 413−421.
(63) Lodge, A. S. *Trans. Faraday Soc.* **1956**, *52*, 120−130.
(64) Tanaka, F.; Edwards, S. F. *Macromolecules* **1992**, *25*, 1516−1523.
(65) Cates, M. E.; Candau, S. J. *J. Phys.: Condens. Matter* **1990**, *2*, 6869−6892.
(66) Turner, M. S.; Cates, M. E. *J. Phys. II France* **1992**, *2*, 503−519.
(67) Turner, M. S.; Marques, C.; Cates, M. E. *Langmuir* **1993**, *9*, 695−701.
(68) Cates, M. E. *Macromolecules* **1987**, *20*, 2289−2296.
(69) For recent reviews of pincer complex chemistry, see: (a) Slagt, M. Q.; van Zwieten, D. A. P.; Moerkerk, A. J. C. M.; Gebbink, R. J. M. K.; Van Koten, G. *Coord. Chem. Rev.* **2004**, *248*, 2275−2282. (b) Albrecht, M.; van Koten, G. *Angew. Chem., Int. Ed.* **2001**, *40*, 3750−3781.
(70) Yount, W. C.; Juwarker, H.; Craig, S. L. *J. Am. Chem. Soc.* **2003**, *125*, 15302−15303.
(71) Yount, W. C.; Loveless, D. M.; Craig, S. L. *Angew. Chem., Int. Ed.* **2005**, *44*, 2746−2748.
(72) Rodriguez, G.; Albrecht, M.; Schoenmaker, J.; Ford, A.; Lutz, M.; Spek, A. L.; va Koten, G. *J. Am. Chem. Soc.* **2002**, *124*, 5127−5138.
(73) Steed, J. W.; Atwood, J. L. *Supramolecular Chemistry*; Wiley: Exeter, 2000.

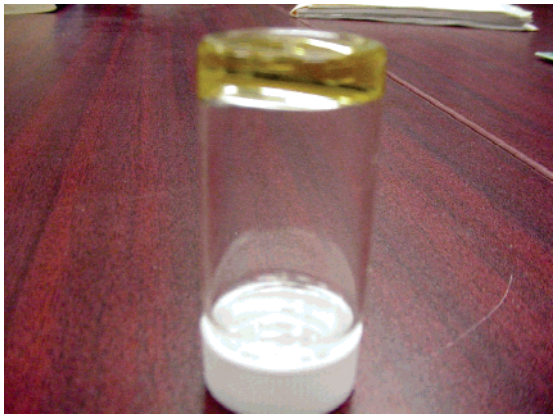

***Figure 3.*** Gel formed from PVP and bimetallic compound **3b** (5% functional group equivalents) at 100 mg/mL in DMSO.

bulk materials and the isolated, coordinative interactions in solution are investigated. The studies on the model compounds and in the bulk materials reveal that the underlying molecular mechanisms of mechanical response are very specific solvent-mediated ligand displacement reactions, and the dynamic mechanical properties are therefore governed by dissociation of the cross-links rather than nondissociative, site-to-site migration. It is the rate at which those cross-links detach and reattach, however, rather than the fraction of time for which they are dissociated, that is the critical determinant of mechanical response. The combination of mechanistic small-molecule studies and macroscopic transient network theories provides a framework by which complex, bulk dynamic mechanical response is not only be explained, but might also be predicted rationally and engineered at the molecular level. Because the dissociation processes in the PVP coordination system are effectively first-order, the same framework applied here is applicable to similar networks comprising common noncovalent interactions such as hydrogen bonds.

## Experimental Section

**Materials.** Dimethylformamide (DMF), dimethyl sulfoxide (DMSO), methylene chloride, pyridine (**2**), (dimethylamino)pyridine (**2b**) (Acros), and poly(4-vinyl pyridine) (PVP) $M_w$ = 60 000 (Aldrich) were used as received. Compounds **1a**−**d** and **3a**−**d** were synthesized as the triflate salts as previously reported.[70,71] The synthesis of the tetrafluoroborate salt of **1b** is reported in the Supporting Information.

**Rheology.** All rheological data were obtained using a Bohlin VOR rheometer with a concentric cylinder geometry (fixed bob and rotating cup). The inner cylinder diameter was 25 mm with an outer cylinder diameter of 26 mm, a bob height of 21.4 mm, and a cone angle of 2.3°. DMSO solutions of PVP and cross-linker **3** (∼2 mL) were annealed three times at 80 °C, cooled to room temperature, and loaded into the cup, with heating when necessary to allow the material to flow into the geometry, and the bob was lowered into the cup. The sample was allowed to equilibrate to 20 °C. Low deformation oscillatory data were obtained at an amplitude of 50% and processed with Bohlin VOR software. Torque bars (98.72 g cm, 10.42 g cm, and 0.245 g cm) were chosen so that the recorded stress moduli were within 10−90% of the dynamic range of the detector.

**Kinetics.** Spin magnetization transfer data were acquired using a 500 MHz Varian NMR with Varian software and a NOESY pulse sequence. A solution of 10 mM **1b** and 20 mM **2a** in DMSO-$d_6$ was made and monitored by 2D $^1$H NMR at 25 °C using the negative intensities generated by the NOESY sequence, which reflect only those contributions due to chemical exchange. The mixing time in the NOESY sequence was varied, and the relative intensities of the irradiated diagonal peaks and those of the cross-peaks between chemically exchanging species were used to calculate $k_f$ and $k_b$ (eq 1).[74]

$$I_{AA}/I_{AB} = [1 + \exp((k_f + k_b)t_m)]/[1 - \exp((k_f + k_b)t_m)] \quad (1)$$

where $I_{AA}$ and $I_{AB}$ are the volume integrals of the diagonal and cross-peaks, respectively, $k_b$ is the reverse rate constant and $k_f$ is the forward rate constant defined by the equilibrium between exchanging species, and $t_m$ is the mixing time. The relative values of $k_b$ and $k_f$ were obtained from the relative concentrations of the exchanging species, measured by $^1$H NMR integration.

***Table 1.*** Equilibrium Constants and Dissociation Rate Constants for Pincer Pd and Pt Complexes **1** with Pyridine (**2**) in DMSO at 25 °C [Uncertainties: $K_{eq}$ (±20%), $k_d$ (±15%)]

| complex | $K_{eq}$ ($M^{-1}$) | $k_d$ ($s^{-1}$) |
|---|---|---|
| **1a·2** | 29[a] | 1450[b] |
| **1b·2** | 33[a] | 17[c] |
| **1c·2** | 8000[a] | 0.026[a] |
| **1d·2** | 4000[a] | 0.0006[a] |

[a] Reference 72. [b] Estimated from the value for **1b·2** following ref 72. [c] Determined by spin magnetization transfer; see text for details.

## Results

**Pyridine Coordination and Exchange: Model System.** We recently reported the thermodynamics and ligand exchange kinetics of pyridine (**2**) coordination to **1a**−**d** in DMSO (Table 1).[70,71] Changes in chemical shifts of either or both **1** and **2** upon coordination allow the thermodynamics to be measured by $^1$H NMR. The structure of the free metal species (that is, metal not coordinated to pyridine) was expected to involve bound DMSO, present in large excess to the triflate counterion, and two series of experiments validate that expectation. First, the association equilibrium constant for **1b·2b** is effectively independent of the concentration of added excess triflate (Supporting Information). Second, replacing triflate with the much more weakly coordinating $BF_4^-$ does not measurably affect the association constant (Supporting Information). Thus, DMSO at effective concentrations of ∼14 M is preferred as a ligand to 3 mM triflate, and the free state of the metal involves coordination to DMSO, as implied in Figure 1. The previously reported thermodynamics (Table 1) are therefore operationally concentration-independent, and they are applicable to networks with different cross-linking percentages, as reported below.

The increased sterics at the metal center have been reported previously to slow the rate of the ligand exchange reactions, as expected for an associative process. The exchange of pyridine ligands underlies the reversibility of the SPs, and, as discussed below, the mechanism of exchange is subtly but importantly tied to a thorough understanding of the bulk dynamic mechanical processes. Two mechanisms for ligand exchange are possible: direct displacement of the first ligand by the second (Figure 2a) or a solvent-assisted exchange (Figure 2b).[75] To gain insight into the mechanism of ligand exchange, the rate of exchange for the bound and free states of ligand **2** was compared to the rate at which the metal complex **1b** changes between ligand-coordinated and solvent-coordinated states. Using spin magnetization transfer, the rate of chemical exchange between the bound and free pyridine ligand was measured to be 16 ± 1 $s^{-1}$

(74) Lee, S.-G. *Magn. Reson. Chem.* **2000**, *38*, 820−822.
(75) Atwood, J. D. *Inorganic and Organometallic Reaction Mechanisms*, 2nd ed.; Wiley-VCH: New York, 1997.

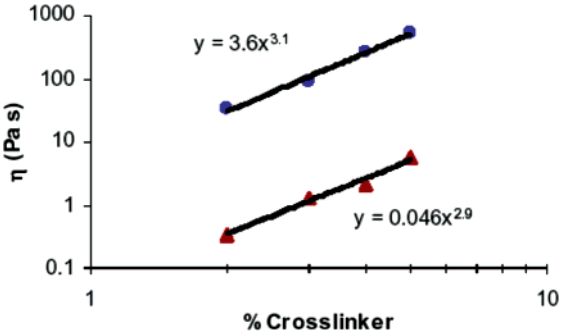


***Figure 4.*** Steady shear viscosity as a function of density of cross-linker **3a** (red ▲) or **3b** (blue ●), expressed as functional group equivalents of metal relative to pyridine side group. 100 mg/mL **3**·PVP in DMSO.

(consistent with an earlier reported value of 15 ± 1 $s^{-1}$), in excellent agreement with a simultaneous measurement of 18 ± 1 $s^{-1}$ for that of the metal complex peak. As shown in Figure 2a, a direct displacement mechanism for ligand exchange would not lead to exchange between bound and free states of protons on the pincer molecule, while in the solvent-assisted pathway (Figure 2b) the pyridine ligand and organometallic pincer complex change states at the same rate. No realistic mechanistic pathways of which we are aware allow metal exchange to occur more rapidly than ligand exchange, and so we treat the two measurements as identical, differing only because of experimental uncertainty. The fact that both species exchange at the same rate indicates that, under the conditions of the experiment, ligand exchange is dominated by the solvent-assisted mechanism, and the rate constant measured for ligand exchange is therefore also the dissociation rate constant $k_d$ (Figure 1), which we hereafter take as the average value of 17 ± 1 $s^{-1}$ for **1b·2**.[76] The same mechanism is observed in the Pt(II) analogues, which exhibit the slower kinetics typical of Pt(II) complexes relative to Pd(II) complexes.[75,77] The pyridine exchange rate of **2**-$d_5$ for **2** in **1d·2**, measured by conventional $^1$H NMR, is effectively independent of the concentration of added **2**-$d_5$ (0.0006 ± 0.0001 $s^{-1}$, Supporting Information), indicating that the solvent-assisted pathway is again the dominant mechanism of ligand exchange. It is certainly possible, and even likely, that at sufficiently high concentrations of free ligand, the direct displacement mechanism would contribute to the ligand exchange rate. As discussed below, however, the dissociation rate constant $k_d$ determined in these measurements is shown to be directly relevant to the mechanism of SP networks.

**Dynamic Mechanical Properties.** We recently reported that mixing dimers **3a**−**d** with poly(4-vinylpyridine) (PVP) in DMSO gives rise to gels of variable thickness (e.g., **3b**·PVP, Figure 3), and control experiments with monomeric metals and competitive inhibition confirmed that associative cross-linking of the PVP chains was responsible for the increased viscosity.[71] At the same 100 mg $mL^{-1}$ concentration in DMSO, PVP alone is not entangled, as revealed by the concentration dependency of the solution viscosity (Supporting Information). The steady shear viscosities of **3a**·PVP and **3b**·PVP are shown as a function of cross-linking density in Figure 4. The steady-shear viscosity of each network scales with (% cross-link)$^3$, a relationship that has been observed previously and one that we discuss below.

(76) This value is revised from that reported previously in ref 71.
(77) Basolo, F.; Pearson, R. G. *Mechanisms of Inorganic Reactions*; Wiley: New York, 1967.

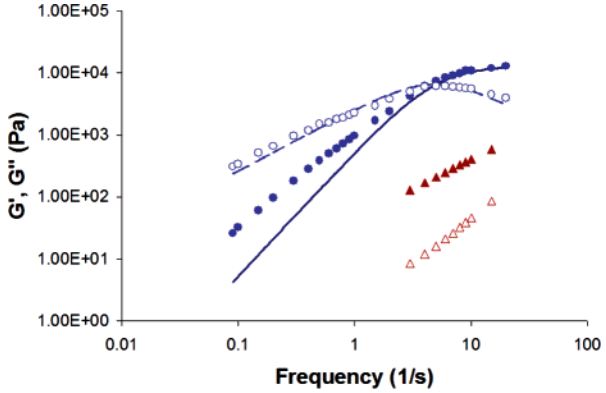


***Figure 5.*** Dynamic moduli for networks of 5% (by functional group) **3a** (red ▲) or **3b** (blue ●) and PVP in DMSO at 100 mg/mL. The storage moduli ($G'$) are shown as filled shapes, while the loss moduli ($G''$) are shown as hollow shapes. The Maxwellian fits for **3b**·PVP are shown as solid lines (blue for $G'$ and black for $G''$); $G_0$ = 13 000 Pa and $\beta$ = 5 $s^{-1}$.

Notably, across all cross-link percentages, the viscosity of **3b**·PVP is a factor of 80−100 higher than that of **3a**·PVP. This ratio agrees reasonably well with that reported previously for 5% cross-linking as measured by the low-frequency plateau in oscillatory shear data. Because the structures and ligand affinities of **3a** and **3b** are so similar, the difference in the viscosities has been attributed directly to the difference in the ligand exchange kinetics of the coordination complexes. As discussed above, the relative rates of pyridine exchange in the model compounds can only be estimated because that of **1a·2** is too fast for the dynamic NMR measurements. The average difference of a factor of 80−100, however, is in good agreement with a difference of 70−100× observed for exchange of (dimethylamino)pyridine **2b** on the same model compounds.

Oscillatory rheology reveals the dynamic mechanical properties of the networks. Representative data are shown for 5% **3a**/**3b** with PVP, 100 mg $mL^{-1}$ in DMSO, in Figure 5. The storage modulus, $G'$, is a measure of the deformation energy that is stored in intact, entropic distortions of the network. The loss modulus, $G''$, is a complementary measure of the deformation energy that is lost, or dissipated as heat, due to relaxations that occur on the time scale of the oscillatory deformations. The frequency dependencies of $G'$ and $G''$ are best discussed in the context of a Maxwell model described by a single relaxation rate $\beta$:

$$G' = G_0(\omega/\beta)^2/(1 + (\omega/\beta)^2) \quad (2)$$

$$G'' = G_0(\omega/\beta)/(1 + (\omega/\beta)^2) \quad (3)$$

where $\beta$ = 5 $s^{-1}$ and $G_0$ =13 000 Pa provide the best fit for PVP·**3b** (shown in Figure 5). The basis of the model is that upon deformation, the associations or entanglements that store stress relax to equilibrium at a rate $\beta$, and so the fraction of surviving, stress-bearing associations falls off with the time scale of the oscillatory deformation. For slow oscillations, $\omega \ll \beta$, and the majority of the deformation energy is dissipated as heat ($G'' > G'$). Conversely, at $\omega \gg \beta$, the majority of stress-bearing cross-links remain intact, $G''$ decreases toward zero, and $G'$ reaches a plateau value $G_0$. It follows from the Maxwell model that $G' = G''$ when $\omega = \beta$, that is, on an experimental time scale at which half of the deformation energy is stored and half is lost through relaxations. The Maxwell fit in Figure 5 deviates

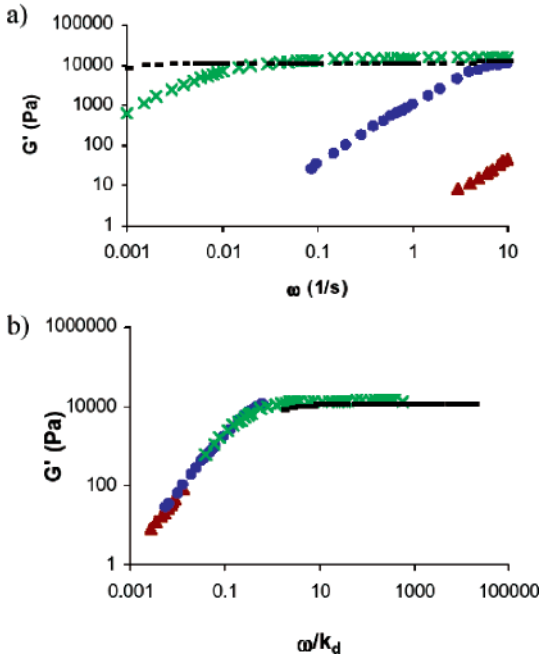


***Figure 6.*** (a) Storage modulus ($G'$) of networks of PVP and 5% **3a** (red ▲), **3b** (blue ●), **3c** (green ×), and **3d** (−) at 100 mg/mL in DMSO at 20 °C. (b) Storage modulus of the same networks as a function of frequency scaled by $k_d$ measured on model complexes **1**·**2**.

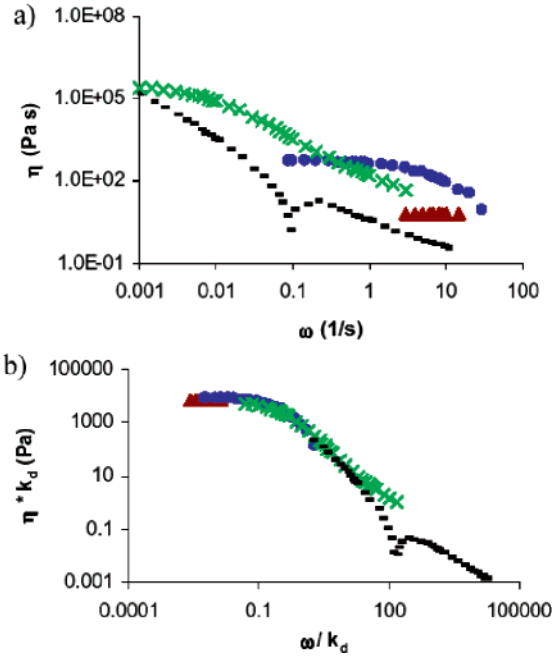


***Figure 7.*** (a) Dynamic viscosity of networks of PVP and 5% **3a** (red ▲), **3b** (blue ●), **3c** (green ×), and **3d** (−) at 100 mg/mL in DMSO at 20 °C. (b) Dynamic viscosities of the same networks scaled by $k_d$ measured on model complexes **1**·**2**.

measurably from the experimental data, and the relaxation dynamics are more complex than can be described quantitatively by a single relaxation rate. The deviation from Maxwell behavior is also manifested in the difference between the observed low-frequency limit of the dynamic viscosity (550 Pa s for **3b**·PVP) and the ratio $G_0/\beta$, taken from the best fit (2600 Pa s); the two would be equal in the limit of perfect Maxwellian behavior.[60] The deviation from Maxwell behavior is at least somewhat general for these systems, in that it is also observed at 2% cross-linking density (Supporting Information). Nonetheless, there is only a single plateau in $G'$ and a single inflection in $G''$ across the range of frequencies accessible, and the simple Maxwell model provides a reasonable basis for discussion.

As seen in Figure 5, the moduli obtained from the oscillatory shear data for **3a**·PVP are shifted to higher frequencies than those of **3b**·PVP. Although the crossing of $G'$ and $G''$ falls outside the range accessible on the rheometer, it can be estimated by scaling against the **3b**·PVP data. The value of $\beta$ thus obtained is 400 $s^{-1}$, a factor of ∼80 greater than that of **3b**·PVP. The change in the relaxation rate of the bulk material is again quantitatively consistent with the expected (70−100)-fold change in the ligand exchange rate of the cross-linker. Similarly, the storage modulus is shifted to progressively lower frequencies for **3c** and **3d**, respectively (Figure 6a), and the dynamic viscosity

$$\eta = G''/\omega \tag{4}$$

is shifted to higher plateau values at low frequency. As the oscillatory frequency $\omega$ reaches a threshold value, $\eta$ begins to decrease with increasing oscillatory frequency. This threshold frequency is also related directly to $\beta$ in the Maxwell eqs 2 and 3, and it occurs at lower values of $\omega$ for the cross-linkers with slower exchange dynamics (Figure 7a).

That these shifts are due to the same, molecular dynamics for all four cases is shown in the scaled fits of Figures 6b, 7b,

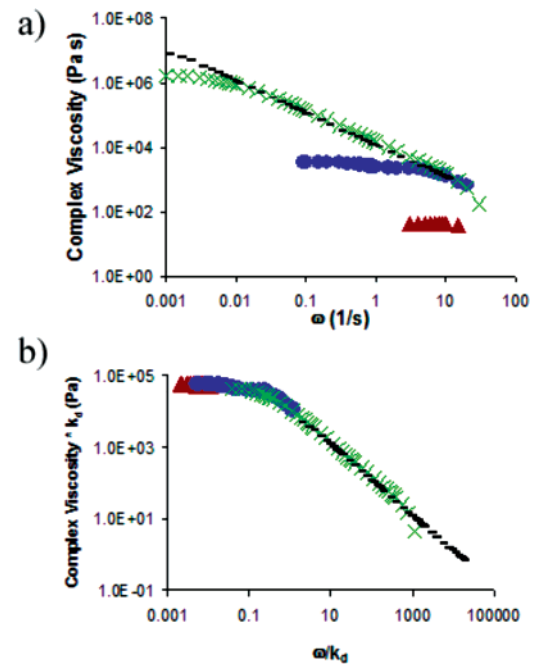


***Figure 8.*** (a) Complex viscosity of networks of PVP and 5% **3a** (red ▲), **3b** (blue ●), **3c** (green ×), and **3d** (−) at 100 mg/mL in DMSO at 20 °C. (b) Complex viscosities of the same networks scaled by $k_d$ measured on model complexes **1**·**2**.

and 8b. When the viscosity is scaled by the ligand dissociation rate $k_d$ taken from the studies reported above for model systems **1**, and the frequency of the applied strain is scaled inversely by the same value, the raw viscosity data of Figure 7a collapse onto the master plot shown in Figure 7b. The excellent scaling is matched when the storage modulus $G'$ is plotted against a similarly scaled frequency in Figure 6b and in the related, scaled complex viscosities of Figure 8b. The differences in bulk viscoelastic behavior, including the deviation from the Maxwell

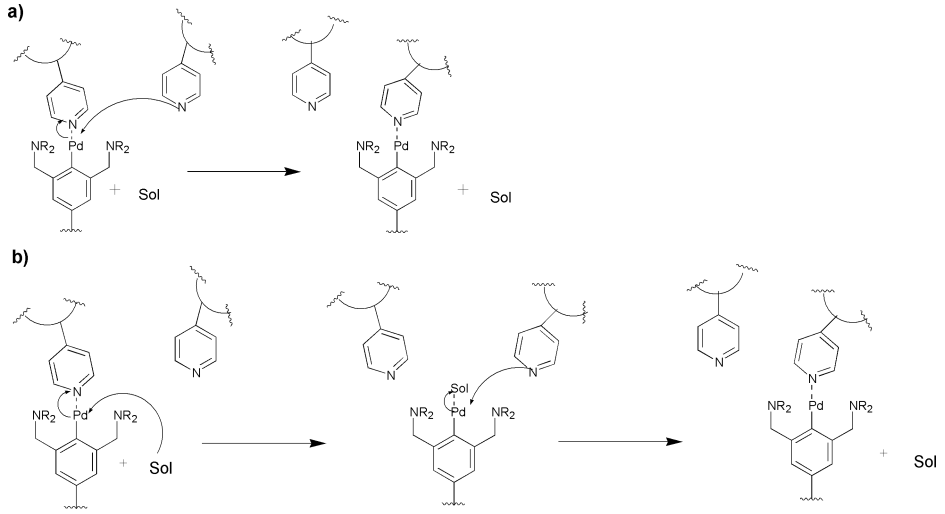


***Figure 9.*** Possible mechanisms of cross-link migration in **3**·PVP networks in DMSO. (a) Direct displacement of one pyridine side chain by another. (b) Solvent-assisted pyridine exchange. Sol represents the DMSO solvent. Positive charges and counterions are not shown.

behavior, are accounted quantitatively by the ligand dissociation rates $k_d$ measured on the model complexes **1**·**2**.

**Mechanism of Network Relaxation.** Cross-link dynamics clearly determine the mechanical properties observed in the steady and oscillatory shear data, and, as with the ligand exchange studies discussed above, there are two molecular mechanisms by which cross-link relaxations might occur (Figure 9): direct displacement and solvent-assisted. Either could, in theory, be operative in these networks. Direct displacement would indicate that a free pyridine of the PVP directly displaces the bound pyridine (Figure 9a), while in the case of solvent-assisted exchange, DMSO would first displace the bound pyridine and, in a second step, a new pyridine would then displace the DMSO (Figure 9b). The implications of these two mechanisms are subtly different. In the case of a direct displacement mechanism, the cross-link remains a part of the network even while it migrates. A solvent-assisted pathway, however, requires that stress relaxation (flow) occur while the cross-link is dissociated from the network.

The mechanistic studies described in a previous section show that the solvent-assisted pathway dominates direct displacement at millimolar concentrations of pyridine. While the excellent scaling of the solvent-assisted dissociation rates and bulk material properties, shown in Figures 6b and 7b, is consistent with a solvent-assisted pathway in the networks, it is not conclusive; steric effects should affect the associative direct displacement pathway as well, and the magnitude of the effect might be quite similar to that of the solvent-assisted pathway. If the solvent-assisted mechanism were also dominant in the networks, however, then the viscosity of the networks would reflect the nucleophilicity of the solvent, and we observe that to be the case. A 5% **3b**·PVP network was formed by mixing the two components at 100 mg $mL^{-1}$ in $CH_2Cl_2$, whose nucleophilicity toward the Pd(II) metal center is much lower than that of DMSO. Upon combining **3b** with PVP in $CH_2Cl_2$, a discrete gel was formed. The gel displayed a much higher viscosity than the DMSO samples, to the extent that it could be picked up and manipulated gently with a spatula for several minutes with only minimal deformation. By comparison, DMF possesses a reasonable ability to serve as a coordinating solvent,

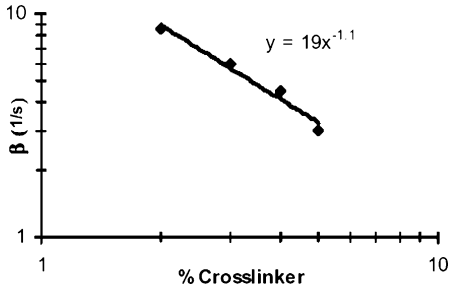


***Figure 10.*** Network relaxation rate $\beta$ as a function of density of cross-linker **3b** in **3b**·PVP, 100 mg $mL^{-1}$ in DMSO, expressed as functional group equivalents of Pd to pyridine.

although it is still less nucleophilic than DMSO.[78] Upon inspection (flow in a tilted vial), the viscosity of 5% **3b**·PVP in DMF was observed to be higher than that in DMSO. The qualitative correlation between viscosity and solvent nucleophilicity suggests that for **3b**·PVP in DMSO, the solvent-assisted pathway dominates ligand exchange in the networks as well as in the isolated organometallic complexes.

Further support for the solvent-assisted pathway is found in the bulk relaxation frequencies $\beta$. The value of $\beta$ derived from the Maxwell models changes as a function of cross-link density, with a power law dependence of $(\text{cross-link})^{-1}$ (Figure 10). That inverse dependence is consistent with transient network models in which not all cross-link dissociation/reassociation events lead to stress relaxation, because of the effect of multiple cross-links along the contour of each PVP.[80] We therefore derive an apparent "intrinsic" relaxation rate $\beta_{int}$ by extrapolating the relaxation rate back to the cross-link density at the gel point, determined by viscosity titrations to be $1.5 \pm 0.17\%$ functional group equivalent. The value of $\beta_{int}$ thus derived is 13 $s^{-1}$ for **3b**·PVP, in good agreement with the solvent-assisted dissociation rate $k_d = 17$ $s^{-1}$, given the subtle electronic and steric differences between PVP and pyridine and the expected contributions of some inactive transitions even at percolation. Each of these effects should slow the displacement of the ligand

(78) Pearson, R. G.; Gray, H. B.; Basolo, F. *J. Am. Chem. Soc.* **1960**, *82*, 787−792.
(79) Rubinstein, M.; Semenov, A. N. *Macromolecules* **1998**, *31*, 1386−1397.
(80) Jongschaap, R. J. J.; Wientjes, R. H. W.; Duits, M. H. G.; Mellema, J. *Macromolecules* **2001**, *34*, 1031−1038.

by DMSO relative to the parent compound. The good agreement between the bulk and molecular rate constants (the scaling relationships of Figures 6b and 7b imply that this agreement is general), while not conclusive, further support a solvent-assisted pathway for network flow and a material relaxation rate that is nearly equivalent to the rate of the solvent-assisted process measured on model compounds.

## Discussion

The results presented above comprise two stories: one a mechanistic study of metal−ligand coordination and ligand exchange, and the other a study of the dynamic mechanical properties of coordinatively cross-linked polymer networks. We are struck by the extent to which the molecular story and the material story are effectively the same. In particular, the scaling of data in the collapsed master plots of Figures 6b and 7b shows that, within experimental uncertainty, a wide range of frequency-dependent dynamic mechanical properties of the networks are determined by the relative kinetics of solvent-assisted ligand exchange as measured on small-molecule model compounds. The extent of the scaling relationship does not necessarily follow from the low-frequency data reported previously,[71] because of the possible presence of alternative relaxation pathways that are not defined by cross-link dissociation. The implications of these results are best discussed in the context of previous theoretical treatments. Two similar classes of theory have been used to describe associative networks similar to the type described here: transient network models and Cates' theory derived for wormlike micelles.

Transient network models are derived from the early work of Green and Tobolsky, who explained the Maxwellian behavior of polymer melts and concentrated polymer solutions through the presence of transient, stress-bearing entanglements whose lifetime corresponds to $1/\beta$ from eqs 2 and 3. The concept is easily extended to associative networks similar to those described in this work, in that the roles of the stress-bearing entanglements are filled by the reversible chemical associations of the cross-links. A typical assumption of these models is that upon dissociation, the stress born by the cross-link is lost, and reassociation occurs to give a network junction that is at equilibrium, at least locally. This assumption may not always be valid, for example, in the case of limited "free" association points investigated by Rubinstein and Semenov,[79] but in general an accompanying feature of transient network theories is that the bond reformation rate contributes to material properties only insofar as it determines $K_{eq}$ (Figure 1) and hence the extent of cross-linking in the network. This intuitively reasonable result has been stated explicitly in theoretical treatments of the problem, for example, by Tanaka and Edwards,[64] but we are aware of no previous experimental studies in which it is addressed directly.

Cates' theoretical work on the viscoelasticity of wormlike micelles[65−68] has been applied previously to linear SPs and SP networks.[3,60] The theory describes "living" wormlike micelle polymers that undergo dynamic scission and reformation along their main chains. The polymers are confined to a reptation tube by the surrounding polymer solution. The entanglements in this case are the physical obstacles defining the tube, but relaxations can occur by dissociation/relaxation/association processes along the wormlike micelle chain. The subtle but important distinction in the Cates theory, relative to transient network models, is that dissociation facilitates conventional polymeric relaxation mechanisms such as reptation or conformational breathing modes. Dissociation need not occur exactly at an entanglement, but only within close enough proximity to an entanglement that, for example, reptation leads to the relaxation of that entanglement and a loss of stress. When the time scale of dissociation is shorter than that of the polymeric relaxation processes, the ultimate relaxation rates are a concatenation of molecular and polymeric dynamics. In the limit that relaxation is dominated by bimolecular "bond interchange" processes, tube effects might be reduced to the extent that the viscoelastic response can be modeled using transient network descriptions.[65,67] The validity of the tube model, even for systems in which the tube itself is dynamic on the time scale of polymer reptation, is dependent on a combination of factors including the specific mechanisms of relaxation within the network.

Although one can imagine morphologies and mechanisms by which the associative networks described here might in principle be aptly described by the Cates theory, contributions from reptation processes are not expected given that DMSO solutions of PVP are not entangled at these concentrations. In practice, we find that transient network models provide a suitable context by which to discuss our results. The absence of obvious contributions from reptation is not surprising. For example, the good agreement between $\beta_{app}$ and $k_d$ is consistent with a purely dissociative relaxation, rather than a concatenation of dissociative and reptative processes. Dissociation is truly "rate determining" with regard to the mechanical properties investigated in this work, as illustrated by direct comparison between networks comprising PVP with different cross-linkers. The cross-links from **3a** and **3b**, for example, spend nearly equivalent fractions of time in their dissociated states; the rates of bond reformation are proportional to the rates of bond dissociation. Nonetheless, the mechanical properties of the networks are adequately explained by considering only the rates of dissociation to the exclusion of the dramatically different reformation rates. The same effect is observed not only by comparing the more tightly binding Pt analogues **3c** and **3d** to each other, it is also observed through the excellent scaling relationships that are valid across all four compounds (Figures 6b, 7b, and 8b). Thus, a central component of transient network theories, that bond reformation rates only affect mechanical properties insofar as they determine what fraction of cross-links are intact, is found here to be quantitatively valid within the experimental uncertainty of our measurements.

Further, the scaling laws observed in our systems are consistent with transient network models. The frequency dependencies of $G'$ and $G''$ are qualitatively consistent with the Maxwell equations, as shown in Figure 5, although there is significant deviation in $G'$ at low frequencies. In addition, the network relaxation rate varies as $\beta \approx (\%\ \text{cross-link})^{-1.0}$, a relationship consistent with the behavior predicted by transient network models developed by Jongschaap et al.[80] In those models, the effects of stochastic cross-links along a polymer chain are treated explicitly by a dynamic interchange between fixed and free states that define polymer segments as active or inactive bearers of stress. Transient network theory further predicts that the steady-shear viscosity $\eta = G_0(1/\beta)$,[61,81] and while the relationship does not hold quantitatively (for 5% **3b**·

PVP, $\eta = 544$ Pa s, in good agreement[82] with the dynamic viscosity of 550 Pa s but also substantially diverged from the computed value of 2600 Pa s), we note that $\eta$ is observed here to vary with (% cross-link)$^{3.0}$. Combining these two relationships, we see that $G_0 \approx$ (% cross-link)$^{2.0}$. The square dependence of $G_0$ is also reasonable, because $G_0$ is proportional to the number of active segments along a chain (proportional to the number of cross-links), and it is also proportional to $1/M_e$, where $M_e$ is the average molecular weight between entanglements and $M_e \approx$ (% cross-link)$^{-1}$ for randomly distributed cross-linkers. Just as rate laws do not prove the mechanism of a chemical reaction, however, scaling laws do not necessarily prove the mechanism of mechanical response. In particular for the case at hand, we note that (1) the transient network and Cates models often exhibit similar scaling laws despite differences in the underlying mechanisms, and (2) the scaling laws could be influenced by the positions of the cross-links within the network. The low-frequency deviations from the Maxwellian description of the storage modulus, such as those observed in Figure 5, might indicate that such effects are not entirely negligible here. Tanaka and Edwards have reported a theoretical treatment of these heterogeneities that is consistent with the observation that the deviation from the Maxwell model also scales with the same, single molecular dissociation rate.[64]

Although neither the exact structure of the networks nor the extent of cooperativity in the associations is known, individual dissociation events clearly dominate the bulk properties. Subsequent investigations might further elucidate the specifics of the relaxation mechanisms, and the family of cross-linkers described in this paper is seemingly well-suited for that purpose. To an extent, the remaining ambiguity highlights the essential result of this work: that despite the complex nature and varied mechanistic possibilities regarding the operative relaxations in the bulk materials, the processes are observed to reflect qualitatively and quantitatively the mechanism and dynamics of exchange in the isolated interactions that as cross-links define the network. Cross-link dissociation, to the exclusion of the rate of reformation, determines the mechanical properties of the materials to the extent that they are investigated here. Not only the steady shear and low-frequency oscillatory viscosity, but also the full dynamic mechanical response of the materials is related by experiment to the kinetics of solvent-mediated displacement of the ligand from the metal. The validity and the potential of this relationship are illustrated succinctly in the scaled master plots of Figures 6b, 7b, and 8b. When entanglements are dominated by engineered, associative cross-links, bulk mechanical properties can be predicted in advance and potentially tuned with reasonable precision by varying the concentrations of individual or mixed cross-linkers that are chosen on the basis of the lifetimes of model association complexes. Although the interactions employed here have substantial covalent character, and ligand exchange is rigorously a bimolecular process, the action of the bulk solvent as both the competitor for metal binding and the enactor of ligand exchange means that the thermodynamics and kinetics of the associations are effectively concentration-independent in a manner that is similar to typical noncovalent reversible interactions such as hydrogen bonds. The ability to intersperse highly specific and well-characterized interactions as defining elements of SP networks therefore holds promise for the rational design of bulk material properties, but, to that end, it will often be the dynamics rather than the thermodynamics of those interactions that require careful consideration.

(81) Annable, T.; Buscall, R.; Ettelaie, R.; Whittlestone, D. *J. Rheol.* **1993**, *37*, 695−726.
(82) As expected from the Cox−Merz rule (see, for example, p 72 of: Barnes, H. A.; Hutton, J. F.; Walters, K. *An Introduction to Rheology*; Elsevier: Amsterdam, 1989), which appears to hold in these systems.

## Conclusion

In conclusion, specific metal−ligand coordination between bis-Pd(II) and Pt(II) organometallic cross-linkers and poly(4-vinylpyridine) in DMSO defines a three-dimensional associative polymer network. The dissociation dynamics of the metal−ligand interaction dominate the dynamic mechanical properties of the networks, both relatively and absolutely, as seen in parameters derived from scaled fits to a Maxwell model of viscoelastic response. The dynamics of the metal−ligand cross-links are governed by solvent-mediated ligand exchange, even given the high (∼1 M) effective concentration of pyridine in the networks. The relaxation rate of the network at percolation is in good quantitative agreement with the rate of solvent-mediated ligand exchange measured in the model systems. Scaling laws agree with transient network models, and reptative relaxations within the network, such as those described in Cates' theory derived for "living" wormlike micelles, need not be invoked to explain the observed dynamics.

The dynamic properties of the bulk materials are quantitatively scaled through the dissociation rates of the cross-links independently of their rates of formation, and so dissociation is effectively equivalent to equilibration. In other words, it is only how frequently, and not for how long, the cross-links dissociate that determines the mechanical response; dissociation is effectively the rate-determining step of the mechanical response. This view leads to simple scaling relationships that unify dynamic mechanical data from four different systems dispersed across several orders of magnitude. A molecular view of the dynamics and mechanism of these associative polymer networks, therefore, is not only qualitatively but also quantitatively relevant to understanding and tailoring the viscoelastic properties of bulk materials. Finally, we note that the methodology employed here might be applicable to a wide range of mechanistic studies into the mechanical properties of associative polymer networks, for example, nonlinear viscoelastic phenomena such as shear-thickening.

**Acknowledgment.** This work was supported the Petroleum Research Fund of the American Chemical Society and Duke University. Partial support was provided by the National Science Foundation, North Carolina Biotechnology Center and Research Corp. D.M.L. is an NSF IGERT Fellow (DGE-0221632). S.L.C. gratefully acknowledges a DuPont Young Professor Award and a Camille and Henry Dreyfus New Faculty Award, and W.C.Y. was supported by a Burroughs Wellcome Fellowship. We thank S. Zauscher for access to his rheometer.

**Supporting Information Available:** Experimental data regarding the effect of counterion binding and synthesis of new compounds. This material is available free of charge via the Internet at http://pubs.acs.org.

JA054298A